Study on Charge Form Factors of the Exotic Nuclei ^{6,8}He*

WANG Zai-Jun[1,2;1)]　　　REN Zhong-Zhou[2,3;2)]

1 (Department of Mathematics, Physics and Information Science,
Tianjin University of Technology and Education, Tianjin 300222, China)
2 (Department of Physics, Nanjing University, Nanjing 210008, China)
3 (Center of Theoretical Nuclear Physics, National Laboratory of Heavy Ion Accelerator of Lanzhou,
Lanzhou 730000, China)

Abstract　Charge radius and charge form factors of different charge density distributions for ^{6,8}He are calculated with the relativistic Eikonal approximation. Detailed comparisons and discussions are presented. It is found that the charge form factors curves of ^{6,8}He are much lower than the experimental ones of ^{4}He. This is, in principle, consistent with the experimental fact. Whereas detailed comparison among the charge form factors which correspond to different charge distributions show significant deviations. This indicates that the effects of the correlations between the halo neutrons and the α-core in ^{6,8}He with different charge density distributions are quite different. This result would provide a useful reference for the possible experiments on the next-generation electron-nucleus collider and for the tests of different theoretical models for the exotic nuclei ^{6,8}He.

Key words　charge form factor, ^{6,8}He, relativistic eikonal approximation, relativistic mean field model

1　Introduction

Recently, it was the first time the root-mean-square charge radius of the exotic neutron-rich nucleus ^{6}He had been precisely measured by L. B. Wang et al. with a model-independent Laser Spectroscopic method[1]. The result is 2.054±0.014fm. The determination of the charge radius of ^{6}He is of particular interest because it can provide new information on the nuclear structure of the lightest two-neutron-halo nuclei. And also the measured result can be used to test various theoretical models for the exotic nuclei ^{6}He. This experimental charge radius is much larger than that of ^{4}He $(1.67\mathrm{fm})^{[2, 3]}$. If we assume that ^{6}He is a system which consists of a α-core and two 1p halo neutrons, the significant difference between the

charge radii of ^{4}He and ^{6}He implies a large spatial fluctuation of the α-core motion with respect to the center of mass and reflects the radial extent of 1p halo neutrons. That is, the exotic nucleus ^{6}He is a loosely bound three-body system. This is in agreement with the experimental results of nuclear reactions.

In recent years, the lightest neutron-halo nuclei ^{6}He and ^{8}He have been extensively studied[4—9]. For light neutron-rich nuclei such as ^{6}He and ^{8}He, one of the widely used models is the few-body model. In this model, by fitting the results of nucleus reactions with the radioactive ion beam at the low and medium energies, the matter density distribution, the neutron density distribution, the proton density distribution and the related root-mean-square (RMS) radii can be extracted. In such a way, various results for ^{6}He and

^{8}He were obtained. In 1992, by analyzing ^{4,6,8}He+C interaction cross sections, the two-neutron and four-neutron removal cross sections[10], Tanihata et al. obtained the proton density distributions for ^{6,8}He,

$$\rho(r) = \frac{2}{\pi^{3/2}} \left\{ \frac{1}{a^3} \exp\left[-\left(\frac{r}{a}\right)^2\right] + \frac{1}{b^3} \frac{Z-2}{3} \left(\frac{r}{b}\right)^2 \exp\left[-\left(\frac{r}{b}\right)^2\right] \right\}, \quad (1)$$

where a=1.397fm and b=2.045fm for ^{6}He, and a=1.431fm and b=1.927fm for ^{8}He. Two years later, Zhukov et al. also obtained a result of proton density distribution for ^{6}He and ^{8}He with the cluster orbital shell model approximation[11—13],

$$\rho(r) = N_c \frac{\exp\left[-\left(\frac{r}{a}\right)^2\right]}{\pi^{3/2} a^3} + N_v \frac{2\, r^2 \exp\left[-\left(\frac{r}{b}\right)^2\right]}{3\pi^{3/2} b^3}, \quad (2)$$

where N_c=2, N_v=0 and a=1.55 for ^{6}He, and N_c=2, N_v=0 and a=1.38 for ^{8}He. In this work, we called densities (1) and (2) the Tanihata density and the Zhukov density, respectively. By reviewing the results of ^{6}He given by Tanihata and Zhukov and comparing them with the experimental data, we find that the results differ very much from each other. This indicates that the reliability of the results obtained by Tanihata and Zhukov should be further tested with more accurate experimental data. Therefore, we calculate the charge radii corresponding to the Tanihata density and the Zhukov density and compare them in the relativistic mean field (RMF) model and with the experimental data. The charge form factors of ^{6}He and ^{8}He are further calculated in the relativistic eikonal approximation[14—17] and compared both with the experimental data of ^{4}He and with each other. The results will provide the tests of the theoretical models for the exotic nuclei in possible experiments on the next-generation electron-nucleus collider[18—23].

This paper is organized in the following way. In Sect. 2, the formalism of the relativistic eikonal approximation for electron scattering and a brief introduction of the RMF model are given. The numerical results and discussions are presented in Sect. 3. A summary is made in Sect. 4.

2　Formalism

2.1　Relativistic eikonal approximation

Eikonal approximation is a widely used method in studying high energy scattering. The eikonal approximation for non-relativistic particles was first developed by Glauber[24], and which now is called the Glauber model. The model was further developed for relativistic particles by Baker in 1964. This model is called the relativistic eikonal approximation in the present paper. Detailed descriptions of this method can be found in Refs. [14] and [15]. Here, we only give a brief introduction.

The elastic differential cross section σ and form factor $F(q)$ in the relativistic eikonal approximation can be expressed as[14]

$$\sigma = \cos^2\left(\frac{1}{2}\theta\right) |I_1(q) + I_2(q)|^2, \quad (3)$$

and

$$|F(q)|^2 = \frac{\sigma}{\sigma_M}, \quad (4)$$

where q is the momentum transfer, σ_M is the Mott cross section. $I_1(q)$ and $I_2(q)$ are given by the following integrals

$$I_1(q) = -\mathrm{i}k \int_0^R J_0(qb)[\mathrm{e}^{2\mathrm{i}\chi(b)} - 1]b\,\mathrm{d}b, \quad (5)$$

$$I_2(q) = -\mathrm{i}k \int_R^\infty J_0(qb)[\mathrm{e}^{2\mathrm{i}\chi(b)} - 1]b\,\mathrm{d}b, \quad (6)$$

where b is the impact parameter, R is the cutoff cylindrical radius, $k = |\boldsymbol{k}_0|$, and J_0 is the Bessel function. For high energy electrons ($E \simeq k$), $\chi(b)$ can be written as[14, 24]

$$\chi(b) = -\frac{1}{2} \int_{-\infty}^\infty V(r)\,\mathrm{d}z, \quad (7)$$

$$r = \sqrt{b^2 + z^2}\ . \quad (8)$$

In the region of $b > R$, since the charge density vanishes beyond R, $V(r)$ can be replaced by the Coulomb potential and $\chi(b)$ can be expressed as a function of the cutoff radius[14, 24]

$$\chi(b) = -\alpha Z \ln\left(\frac{b}{R}\right). \quad (9)$$

In the region of $b < R$, $\chi(b)$ is given by[14]

$$\chi(b) = -Z\alpha \log\left(\frac{b}{R}\right) - 4\pi\alpha \int_b^R r^2 \rho(r) y\left(\frac{b}{r}\right)\mathrm{d}r, \quad (10)$$

where

$$y(x) = \log\left[\frac{1 + (1-x^2)^{\frac{1}{2}}}{x}\right] - (1-x^2)^{\frac{1}{2}}, \qquad (11)$$

and $\rho(r)$ is the charge density distribution, which satisfies the following normalization relation

$$\int \rho(r)\mathrm{d}\boldsymbol{r} = Z . \qquad (12)$$

Since we are concentrating on the high-energy electron scattering off light nucleus, the recoil effect must be taken into account. This can be done by dividing the cross section by a factor

$$f_{\mathrm{rec}} = \left(1 + \frac{2E\sin^2\dfrac{\theta}{2}}{Mc^2}\right). \qquad (13)$$

Also we replace the momentum transfer q by the effective momentum transfer q_{eff},

$$q_{\mathrm{eff}} = q(1 + 1.5\,\alpha\,Z\hbar c/(E\,R_0)), \qquad (14)$$

in our calculation which takes into account the fact that the electron is attracted by the Coulomb potential. In Eq. (14), $R_0 = 1.07A^{1/3}$, A is the mass number of the nucleus.

The Eqs. (3) — (12) together with the corrections (13) and (14) enable us to predict the form factor for a given charge density distribution. In order to calculate the charge form factors corresponding to the proton densities given by Tanihata and Zhukov, we must transfer the proton density distributions into charge density distributions by folding the former with the proton charge density distribution. The following form of the proton charge form factor[25] is used in the calculation.

$$F_{\mathrm{p}}(q) = \sum_{i=1}^{4}\frac{a_i}{1 + \dfrac{q^2}{b_i}} , \qquad (15)$$

where $a_1 = 0.312$, $a_2 = 1.312$, $a_3 = -0.709$, $a_4 = 0.085$, $b_1 = 6.0$, $b_2 = 15.02$, $b_3 = 44.08$ and $b_4 = 154.2$.

2.2 The relativistic mean-field model

Since the RMF model is a standard theory and the details can be found in many works[26—29], we only give the main elements here. The starting point of this model is an effective Lagrange density $\mathscr{L}$ for interacting nucleons, the σ, ω, ρ mesons, and photons,

$$\begin{aligned}
\mathscr{L} ={}& \bar{\Psi}(\mathrm{i}\gamma^\mu\,\partial_\mu - m)\Psi - g_\sigma\bar{\Psi}\sigma\Psi - g_\omega\bar{\Psi}\gamma^\mu\omega_\mu\Psi - \\
& g_\rho\bar{\Psi}\gamma^\mu\rho_\mu^a\tau^a\Psi + \frac{1}{2}\partial^\mu\sigma\partial_\mu\sigma - \frac{1}{2}m_\sigma^2\sigma^2 - \frac{1}{3}g_2\sigma^3 - \\
& \frac{1}{4}g_3\sigma^4 - \frac{1}{4}\Omega^{\mu\nu}\Omega_{\mu\nu} + \frac{1}{2}m_\omega^2\omega^\mu\omega_\mu + \frac{1}{4}c_3(\omega_\mu\omega^\mu)^2 - \\
& \frac{1}{4}R^{a\mu\nu}\cdot R_{\mu\nu}^a + \frac{1}{2}m_\rho^2\rho^{a\mu}\cdot\rho_\mu^a - \frac{1}{4}F^{\mu\nu}F_{\mu\nu} - \\
& e\bar{\Psi}\gamma^\mu A_\mu\frac{1}{2}(1-\tau^3)\Psi,
\end{aligned} \qquad (16)$$

with

$$\Omega^{\mu\nu} = \partial^\mu\omega^\nu - \partial^\nu\omega^\mu, \qquad (17)$$

$$R^{a\mu\nu} = \partial^\mu\rho^{a\nu} - \partial^\nu\rho^{a\mu}, \qquad (18)$$

$$F^{\mu\nu} = \partial^\mu A^\nu - \partial^\nu A^\mu, \qquad (19)$$

where the meson fields are denoted by σ, ω_μ, and ρ_μ^a and their masses are denoted by m_σ, m_ω, and m_ρ, respectively. The nucleon field and the rest mass are denoted by Ψ and m, respectively. A_μ is the photon field which is responsible for the electromagnetic interaction and $\alpha = 1/137$. The effective strengths of the coupling between the mesons and nucleons are, respectively, g_σ, g_ω, and g_ρ. g_2 and g_3 are the nonlinear coupling strengths of the σ meson. c_3 is the self-coupling term of the ω field. The isospin Pauli matrices are written as τ^a, with τ^3 being the third component.

Under the no-sea approximation and the mean-field approximation, a set of coupled equations for mesons and nucleons can easily be obtained by the variational principle[31—34]. This set of equations can be solved consistently by iterations. After a final solution is obtained, we can calculate the binding energies, root-mean-square radii of proton, neutron density distributions and single particle levels. The details of numerical calculations are described in Refs. [24] and [25].

The relativistic mean field (RFM) model is a many-body theory, so it is usually considered to be valid to the medium and heavy nuclei. When it is applied to light nuclei such as ^{6,8}He, much care should be taken. In Ref. [4], the RMF theory with the NL1 parameter set was used in studying the halo structure of ^{6,8}He. It was found that the result is in good

agreement with the ones from the other models. We also employed the RFM theory with another parameter set, the NL-SH parameters, to study ^{6,8}He. It was found that the binding energies for ^{6,8}He and the charge radius for ^{6}He agree with the experimental results very well. Therefore, it would seem to make sense that one can use the RFM theory together with the relativistic eikonal approximation to predict of the charge form factors for ^{6,8}He and compare the results with those calculated by using the Tanihata density and the Zhukov density.

3 Numerical results and discussions

To begin with, we calculated the charge radii for ^{6,8}He by using the Tanihata density, the Zhukov density and the RMF model. The results are listed in Table 1. In the table, r_c is the RMS charge radius and BE denotes the binding energy. For convenience, we also list the experimental charge radius and binding energy of ^{4}He[2, 35] in the last column.

The experimental binding energies for ^{6,8}He are, respectively, 29.268MeV and 31.408MeV, and the measured charge radius for ^{6}He is 2.054±0.014fm[1]. By comparing the RMF results with the experimental data of ^{6,8}He, it is found that the RMF model can reproduce the experimental data very well. To check the stability of the RMF model for light nuclei, we also study the neighboring nuclei ^{6,7}Li, ^{9}Be, ^{10}B with the RMF model (results are not shown here). We find that the calculated binding energies and charge radii are all in agreement with the experimental results well. This shows that the RMF model is valid for the light nuclei such as ^{6,8}He, ^{6,7}Li, ^{9}Be and ^{10}B.

Table 1. Charge radii of ^{6,8}He from different charge densities, the experimental results for ^{4}He and the binding energies for ^{6,8}He from the RMF model.

	^{6}He			^{8}He			^{4}He
	Tanihata	Zhukov	RMF	Tanihata	Zhukov	RMF	Exp.
r_c/fm	1.921	2.085	2.029	1.953	1.899	2.0384	1.676
BE/MeV			28.629			31.796	28.296

Based on the validity of the RMF model for ^{6,8}He, we compare the charge radii of ^{6}He listed in Table 1. On the one hand, it can be seen from the table that the charge radii corresponding to the Tanihata density, the Zhukove density and the RMF model are all much larger than that of ^{4}He ($\Delta r_c \geqslant 0.21$fm). This in principle agrees with the experimental fact. On the other hand, there exist yet significant differences among the results for ^{6}He. The RMF charge radius for ^{6}He agrees with the experimental one best. The charge radius of ^{6}He corresponding to Tanihata density has the largest deviation from experimental one. The RMF charge radius for ^{8}He is 2.0384fm which is slightly larger than that for ^{6}He. This holds true for the charge radii of ^{6,8}He corresponding to the Tanihata density. Whereas the results of ^{6,8}He corresponding to the Zhukov density have opposite behavior. These differences call for further experimental studies of ^{6,8}He so that the theoretical models can be tested. It is well known that electron-nucleus scattering is one of the most powerful tool to study the nuclear charge distribution. For the sake of comparison with the possible experiments in the colliding electron-exotic nucleus storage ring[19], we further calculate the charge form factors of ^{6,8}He corresponding to the Tanihata density, the Zhukov density and the RMF charge distribution within the relativistic Eikonal approximation. The results are shown in Figs. 1—4.

In Fig. 1 we compare the calculated charge form factors of ^{6}He with the experimental ones of ^{4}He. The solid and dashed curves are the form factors corresponding to the Tanihata density and the Zhukov density for ^{6}He, respectively. The dotted curve represents the charge form factor for ^{6}He in the RMF model. The filled circles denote the experimental charge form factor for ^{4}He and the dash-dotted curve describes the results calculated by using the experimental charge distribution of ^{4}He[36, 37]. It is seen from this figure that there are two important features about the charge form factors. The first is that the variational tendency of the changes of the ^{6}He charge
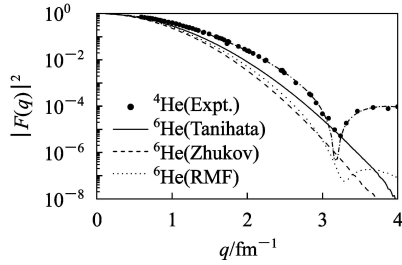
Fig. 1. Comparison of charge form factors between ^{4}He and ^{6}He. For ^{4}He, the filled circles are experimental data[36], the dash-dotted curve is the result from the experimental charge distribution[37]. For ^{6}He, the solid, dashed and dotted curves correspond to the Tanihata density, the Zhukov density and the RMF charge distribution, respectively.

form factors corresponding to different densities are generally in consistent with each other. They are all much lower than that of ^{4}He. This implies that the charge radius of ^{6}He is much larger than that of ^{4}He, and the charge density near the center of ^{6}He is lower than that of ^{4}He. This is in agreement with the experimental facts. From the viewpoint of few-body model, this can be understood, because both the motions of the α-core and the two $1p$ neutrons with respect to the ^{6}He c.m. have a large spatial expansion. The differences in charge form factor between ^{6}He and ^{4}He can also be explained by the many-body theory. Since there exist correlations among the nucleons within a nucleus, the two $1p$ halo neutrons in ^{6}He will 'drag' the two $1s$ protons outward and this leads to a large charge extension and a large charge radius. Thus, it could be concluded that no matter whether the few-body model or the many-body model is used, the difference of the charge form factors between ^{6}He and ^{4}He reflects the correlations between the halo neutrons and the α-core or the $1s$ protons in ^{6}He. The second important feature is that there exist significant discrepancies among the charge form factors of ^{6}He in different density cases. Firstly, in the RMF model, there is a minimum around $q = 3.25\text{fm}^{-1}$, which is similar to that of ^{4}He. Whereas for charge form factors in the Tanihata density and Zhukov density cases, no minimum appear in the charge form factor curve within the range of the considered momentum transfer. This shows that the surface of the charge distribution produced in the RMF

model is sharper than those in the Tanihata density and Zhukov density cases. Secondly, the charge form factor curve corresponding to the Zhukov density is much lower than that corresponding to the Tanihata density. This indicates that around the center of nuclei, the charge density given by Zhukov is lower than that given by Tanihata. These differences imply that the correlations between the halo neutrons and the α-core or the $1s$ protons in different density cases are quite different.

Figure 2 shows the comparison of the charge form factors for ^{8}He calculated by using the Tanihata density, the Zhukov density and the RMF model charge density and the experimental ones of ^{4}He. The same conclusions as we have made about Fig. 1 hold for Fig. 2 except the following fact. In Fig. 1 the ^{6}He charge form factor curve corresponding to the Zhukov density is much lower than that calculated by using the Tanihata density. While for ^{8}He, the results in these two density cases are very close, but the order of the curves is reversed (see Fig. 2). This difference shows that for ^{8}He the strengths of the correlation between the halo neutrons and the α-core in the Tanihata density and Zhukov density cases are very close, while that for ^{6}He the corresponding strengths have relatively larger difference and even opposite effects.

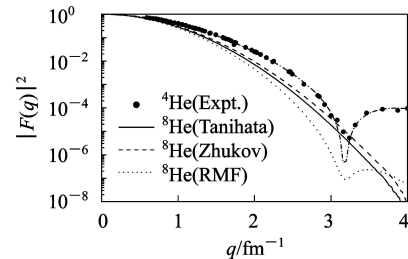Fig. 2. Comparison of charge form factors between ^{4}He and ^{8}He. For ^{4}He, the filled circles are experimental data[36], the dash-dotted curve is the results from the experimental charge distribution[37]. For ^{8}He, the solid curve corresponds to the Tanihata density, the dashed curve corresponds to the Zhukov density, and the dotted curve corresponds to the RMF charge distribution.

In Fig. 3, we compare the charge form factors of ^{6,8}He calculated by using the Tanihata density and the RMF charge distribution. It is seen that the charge form factors of ^{6}He (solid curve) and ^{8}He

(dashed curve) in the Tanihata density case are very close. The charge form factor curves of ^{8}He are only slightly lower than those of ^{6}He. This indicates that

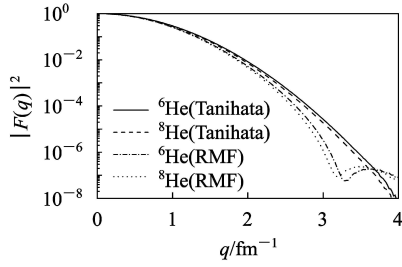Fig. 3. Comparison of charge form factors between ^{6}He and ^{8}He. For ^{6}He, the solid curve corresponds to the Tanihata density, the dash-dotted curve corresponds to the RMF charge distribution. For ^{8}He, the dashed curve corresponds to the Tanihata density and the dotted curve corresponds to the RMF charge distribution.

the charge distributions for ^{6}He and ^{8}He given by Tanihata are almost the same. This means that when two $1p$ neutrons are added to ^{6}He, the motions of two $1s$ protons are not much disturbed. The same conclusion can be drawn by comparing the charge form factors by using the RMF model charge distribution for ^{6}He and ^{8}He. But this conclusion does not hold for ^{6}He and ^{8}He with the Zhukov density, because a large discrepancy between the charge form factors of ^{6}He and ^{8}He is not only in the magnitude but also in their order (see Figs. 4 and 5). In Fig. 5, we contrast the charge form factors for ^{6}He and ^{8}He. The solid and dashed curves are the results with the Tanihata density for ^{6}He and ^{8}He, respectively, and the dotted and short-dash dotted curves correspond, respectively, to the results for ^{6}He and ^{8}He with the Zhukov density. At first sight, we can see that the curves are divided into two groups, one group consists of three curves (the solid, dashed, and short-dash dotted curves, corresponding respectively to the charge form factors of ^{6}He and ^{8}He given in the Tanihata density case and that of ^{8}He given in the Zhukov density case), and another is composed of the dotted curve only. Namely, the charge form factors for ^{8}He given by the Tanihata density and Zhukov density and for ^{6}He given by the Tanihata density are roughly the same. While for ^{6}He, those with the Tanihata density and Zhukov density are different. One can further find that the charge

form factor curve for ^{8}He given by the Tanihata density is slightly lower than that for ^{6}He with the same density distribution. Whereas in the Zhukov density case, the tendency of the changes of the charge form factors for ^{6}He and ^{8}He with respect to the momentum transfer are very different. The charge form factor curve for ^{8}He is much higher than that for ^{6}He,
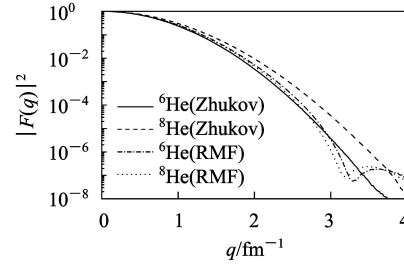

Fig. 4. Comparison of charge form factors between ^{6}He and ^{8}He. For ^{6}He, the solid curve corresponds to the Zhukov density, the dash-dotted curve corresponds to the RMF charge distribution. For ^{8}He, the dashed curve corresponds to the Zhukov density and the dotted curve corresponds to the RMF charge distribution.
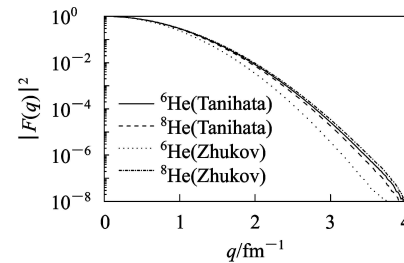

Fig. 5. Comparison of charge form factors for ^{6}He and ^{8}He. For ^{6}He, the solid curve corresponds to the Tanihata density and the dotted curve corresponds to the Zhukov charge distribution. For ^{8}He, the dashed curve corresponds to the Tanihata density and the short-dash dotted curve corresponds to the Zhukov charge distribution.

which is in great contrast with the results in the Tanihata density case. The difference between the Tanihata and Zhukov densities can also be noticed from the expressions (1) and (2) presented in the Introduction. The models used by Tanihata and Zhukov for ^{6}He and ^{8}He happen to be exactly the same, but the values taken by the only parameter a are different. The values of a for ^{8}He in these two densities cases are respectively 1.431fm and 1.38fm and for ^{6}He given

by Tanihata is 1.397fm, and they do not differ much. But the value of a for ^{6}He given by Zhukov, which is 1.55fm, is much greater than that given by Tanihata. This large contrast between the charge densities, and consequently, the charge form factors show that both densities may contain opposite effects of the correlation between the halo neutrons and the α-core on the charge density distributions in ^{6}He and ^{8}He.

Besides, the one-parameter gaussian model is somewhat too simple for describing the density distributions for real nuclei like ^{6}He and ^{8}He because the gaussian model can not produce the minimums of the form factors which appear in all of the nuclei whose charge form factors have experimentally been measured except for the nucleus of hydrogen, the proton. Therefore, it is necessary to investigate ^{6}He and ^{8}He to clear up these contradictions.

4   Conclusion

In summary, we calculate the charge radii and charge form factors for ^{6}He and ^{8}He by using the Tanihata density, the Zhukov density and the RMF model. Comparisons and discussions are made. It is found that the charge form factor curves for ^{6,8}He are much lower than the experimental ones of ^{4}He. This is in principle consistent with experiments. But there is still much left to be clarified. The charge radii and charge form factors with different models for the same nucleus differ from each other very much. There may exist even opposite effect of the correlation between the halo neutrons and the α-core on the charge density distributions in ^{6}He and ^{8}He. Thus, it is desirable to carry out more accurate investigations on ^{6}He and ^{8}He. Electron scattering is one of the most effective tools to provide information on nuclear charge density distributions. Therefore, it will be of interest to study ^{6,8}He on the next-generation electron-nucleus collider[18—22] and compare the experimental data with the results given in this work.

References

1 WANG L B, Mueller P, Bailey K et al. Phys. Rev. Lett., 2004, **93**: 142501

2 de Vries H, de Jager C W, de Vries C. At. Data Nucl. Data Tables, 1987, **36**: 495

3 Borie E, Rinker G A. Phys. Rev., 1978, **A18**: 324

4 LI Zhi-Hong, LIU Wei-Ping, BAI Xi-Xiang et al. Phys. Lett., 2002, **B527**: 50

5 LIU Zu-Hua et al. Phys. Rev., 2003, **C68**: 024305

6 YE Yan-Lin, PANG Dan-Yang et al. Phys. Rev., 2005, **C71**: 014604

7 CHEN Bao-Qiu. HEP & NP, 1999, **23**: 807 (in Chinese) (陈宝秋. 高能物理与核物理, 1999, **23**: 807)

8 LIU Zu-Hua et al. HEP & NP, 2002, **26**: 696 (in Chinese) (刘祖华等. 高能物理与核物理, 2002, **26**: 696)

9 LIU Zu-Hua et al. HEP & NP, 2003, **27**: 135 (in Chinese) (刘祖华等. 高能物理与核物理, 2003, **27**: 135)

10 Tanihata I, Hirata D, Kobayashi T et al. Phys. Lett., 1992, **B289**: 261

11 Zhukov M V, Korsheninnikov A A, Smedberg M H. Phys. Rev., 1994, **C50**: R1

12 Korsheninnikov A A, Nikolskii E Yu, Bertulani C A et al. Nucl. Phys., 1997, **A617**: 45

13 Korsheninnikov A A, Kuzmin E A, Nikolskii E Yu et al. Nucl. Phys., 1997, **A616**: 189c

14 Baker A. Phys. Rev., 1964, **134**: B240

15 WANG Zai-Jun, REN Zhong-Zhou. Phys. Rev., 2004, **C70**: 034303

16 WANG Zai-Jun, REN Zhong-Zhou. Phys. Rev., 2005, **C71**: 054323

17 WANG Zai-Jun, REN Zhong-Zhou, FAN Ying. Phys. Rev., 2006, **C73**: 014610

18 Casten R F, Sherrill B M. Prog. Part. Nucl. Phys., 2000, **45**: S171

19 Suda T, Maruyama K, Tanihata I. RIKEN Accel. Prog. Rep., 2001, **34**: 49

20 Suda T. Proceedings of the International Workshop XXXII on Gross Properties of Nuclei and Nuclear Excitations. Edited by Buballa M, Knoll J, Nörenberg W et al. Hirschegg, Austria, 2004. 235

21 An International Accelerator Facility for Beams of Ions and Antiprotons. GSI Report, 2002

22 Simon H. Proceedings of the International Workshop XXXII on Gross Properties of Nuclei and Nuclear Excitations. Edited by Buballa M, Knoll J, Nörenberg W et al. Hirschegg, Austria, 2004. 290

23 MA Er-Jun, MA Yu-Gang, CHEN Jin-Gen et al. Chin. Phys. Lett., 2006, **23**: 2695

24 Glauber R. J. Lectures in Theoretical Physics, Vol. I. New York: Interscience Publishers, 1959

25 Simon G G et al. Nucl. Phys., 1980, **A333**: 381

26 Gambhir Y K, Ring P, Thimet A. Ann. Phys. (N.Y.), 1990, **198**: 132

27　Horowitz C J, Serot B D. Nucl. Phys., 1981, **A368**: 503

28　MA Zhong-Yu, SHI Hua-Lin, CHEN Bao-Qiu. Phys. Rev., 1994, **C50**: 3170

29　REN Zhong-Zhou, Mittig W, Sarazin F. Nucl. Phys., 1999, **A652**: 250

30　REN Zhong-Zhou, Mittig W, CHEN Bao-Qiu et al. Phys. Rev., 1995, **C52**: R20

31　Ring P. Prog. Part. Nucl. Phys., 1996, **37**: 139

32　Warrier L S, Gambhir Y K. Phys. Rev., 1994, **C49**: 871

33　Tanihata I, Hirata D, Kobayashi T et al. Phys. Lett., 1992, **B289**: 261

34　Hirata D, Toki H, Tanihata I et al. Phys. Lett., 1993, **B314**: 168

35　Audi G, Wapstra A H. Nucl. Phys., 1993, **A565**: 1

36　Frosch R F et al. Phys. Rev., 1967, **160**: 874

37　Arnold R G et al. Phys. Rev. Lett., 1978, **40**: 1429

奇特原子核^{6,8}He的电荷形状因子研究*

王再军$^{1,2;1)}$　　任中洲$^{2,3;2)}$

1 (天津工程师范学院数理系　天津　300222)
2 (南京大学物理系　南京　210008)
3 (兰州重离子加速器国家实验室原子核理论中心　兰州　730000)

摘要　应用相对论Eikonal近似计算了用不同模型给出的 ^{6,8}He 的电荷半径和电荷分布的形状因子, 并将结果与 ^{6}He和^{4}He的实验结果进行了比较. 结果显示不同模型给出的电荷半径和电荷形状因子差别很大, 表明不同模型给出的晕中子与 α 核芯的关联有很大的差异. 计算和讨论结果为在下一代电子–原子核对撞机上可能进行的实验提供了理论参考, 同时, 也为现有讨论奇特原子核的理论模型提供了检验.

关键词　电荷形状因子　^{6,8}He　相对论Eikonal近似　相对论平均场模型